Proceedings of the 2nd International Conference on Computing Innovation and Applied Physics (CONF-CIAP 2023)
DOI: 10.54254/2753-8818/5/20230446

Assistive technology control using eeg signal

Changyang Gui[1]

[1]School of Electrical Engineering and Telecommunication, University of New South Wales, Sydney, 2052, Australia

changyang.gui@student.unsw.edu.au

Abstract. Australian Institute of Health and Welfare states that about 18% of people in Australia, which is 4.4 million, suffers disability. Hosseini et al argued that physically disabled people experience more restrictions in social activities than healthy people, which are associated with lower level of well-being and poor quality of life. To improve the life quality of disabled people, a study is carried out to determine an effective and accurate way to realize what disabled people think. Although there are similar products been made, the previous built products are heavy, clunky, slow in response and inaccurate. In order to solve the problem, an integrated circuit (IC) with a microcontroller is used instead of a laptop and a control system is also implemented to accelerate the response and improve the accuracy. An isolating circuit is implemented as well to improve the stability and durability of the system. Experiment result shows that the IC implemented weighs around 5g, which is 400 times lighter comparing with previous products. The deviation is controlled to be within 2% and the response time is measured to be 0.5s the power consumption is measured to be less than 100μW, which is well within the budget.

Keywords: assistive technology, robotic arm, integrated circuit, control system.

1. Introduction

According to Australian Institute of Health and Welfare, there are over 4.4 million people with some form of disability in Australia [1]. The disability has greatly affected disabled people's life quality as although the brain can send command to the muscles, it cannot be moved due to disability Therefore, it is essential to design a system that can allow disabled people to do what cannot be done before due to disability such as grabbing a coffee cup for an armless man. In order to achieve that, a system consist of two parts are designed. The first part is electroencephalography (EEG) signal acquisition and processing, which is aimed to get the EEG signal from the patient's brain, filter out the noise and correctly interpret the signal to the move the patient commanded. The first part mainly consists of a low-noise amplifier to amplify the weak EEG signal, an analogue-to-digital converter to convert the analogue EEG signal to digital signal, a notch filter and a lowpass filter to eliminate the noises which could affect the subsequent process, and an isolation circuit for protection purpose. A sophisticated machine learning algorithm is implemented to interpret the filtered signal obtained from the processes mentioned before. However, due to the focus of this paper, the machine learning algorithm is not covered in detail. A microcontroller is used to send commands to the robotic arm given the interpreted EEG signal. For the second part, the robotic arm could be modelled as a DC motor, as the output of the microcontroller is not strong enough to directly power a DC motor, a motor driver is implemented to provide the high power needed by the motor taken the small voltage signal from the microcontroller. A motor control system is also used to ensure the smooth, accurate and fast response of the motor to improve the response time and accuracy. By designing such a system, the life quality of the disabled people could potentially be dramatically increased and also it could be a catalyst for the assistive technology industry where more scientists could be motivated to conduct more thorough research on the related field to improve the disabled people's life quality.

2. System description

The system consists of two major parts, which are EEG Signal Acquisition and Processing, and Robotic Arm Driver and Control. The first part is responsible for gathering the EEG signals and converting the gathered signal into control signal. The control signal will be then sent to the second part to drive and control the robotic arm. Due to the higher stability and lower transmission time, a wired connection is chosen to implement the system. The system block diagram is shown below in Figure 1.

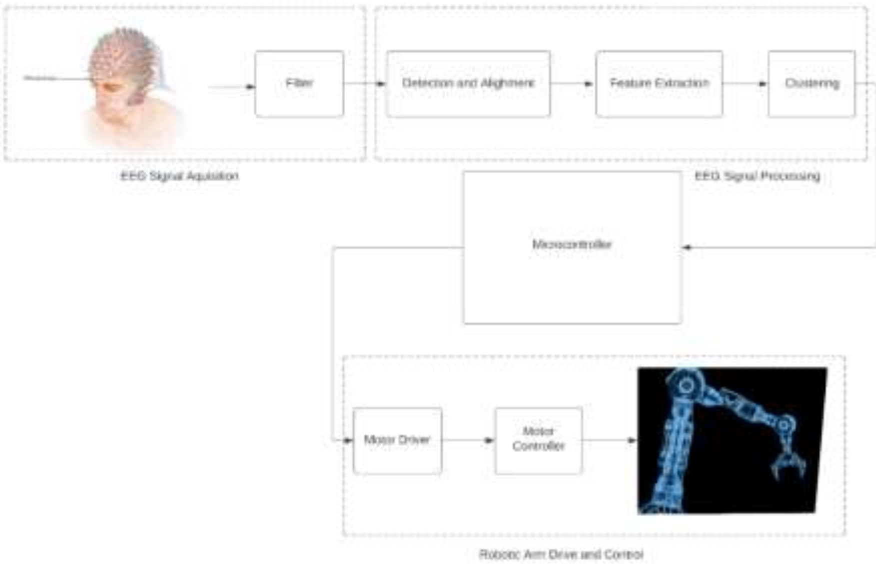

Figure 1. System Description.

The EEG signal processing part is not in the scope of this project as the project is mainly focused on the control system design. In terms of the EEG Signal Processing part, the current solution is to use supervised software processing, which is time-consuming, complex, and highly subjective. So, it is better to implement an unsupervised hardware processing method in the future with Ultra-low-power implantable real-time Application Specified Integrated Circuit (ASIC) and accelerated (~10,000×) Field-Programmable Gate Array (FPGA) data analysis.

2.1. EEG Signal acquisition and processing

2.1.1. Amplifying, filtering and analogue-to-digital converting. As the neural signal from the brain is relatively weak with a magnitude of approximately 0.1mV, an amplifier was implemented to amplify the signal for further analysis. To minimise the impact of noise on the signal, a low-noise amplifier (LNA) was implemented. An LNA is an amplifier that amplifies a low-power signal without significantly decrease its signal-to-noise ratio (SNR). An amplifier will not only increase the power of the signal, but also the noise present at the input, moreover, the amplifier also introduces additional noise. LNAs are designed to minimize that additional noise introduced by using low-noise components. AD8055 LNA was implemented due to its low input-referred noise density of $6\mathrm{nV}/\sqrt{\mathrm{Hz}}$, low power consumption of 65mW and well documentation. The sample amplifier implementation with a gain of 10 is shown below in Figure 2.

DOI: 10.54254/2753-8818/5/20230446

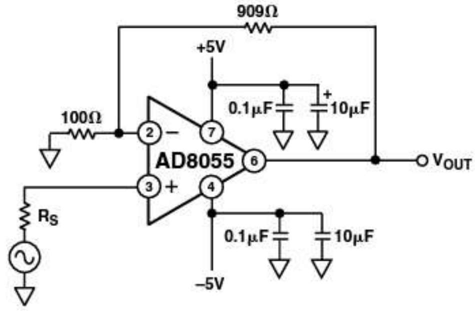

Figure 2. LNA Sample implementation.

As the signal must be amplified to the level of around $0.5V$ for subsequent processing, the gain needs to be set to $5kV/V$, which indicates the feedback resistance need to be set to $499.9k\Omega$ while keeping the input resistance unchanged.

As the EEG signal is an analogue signal, which could not be interpreted by the microcontroller, therefore, an analogue-to-digital converter (ADC) is needed to convert the EEG signal to digital signal. In order to maintain as much information as possible, the ADC chosen needs to have high resolution, which indicates high sampling rate and high effective-number-of-bits (ENOB). Therefore, the $AD7322$ ADC was chosen to implement due to its 12-bit resolution, 8-bit ENOB, high signal-to-noise ratio (SNR) of $76dB$, fast processing speed with a delay of maximum $26ns$, low power consumption of $30mW$ and its well documentation. The functional block diagram is shown in Figure 3 below.

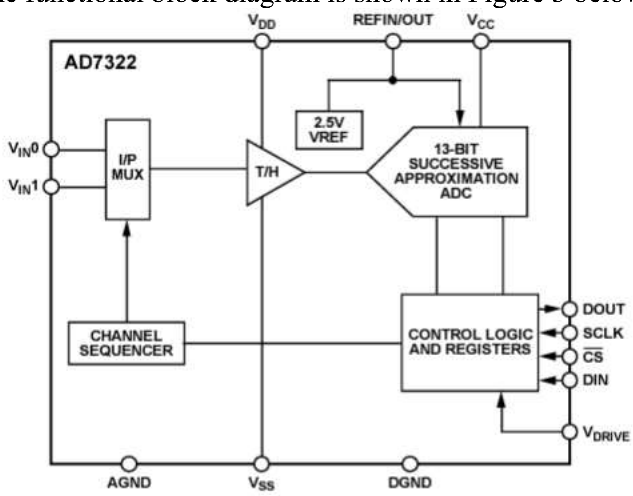

Figure 3. Functional Block Diagram of AD7322.

The $AD7322$ is designed on $iCMOS$ (industrial Complementary Metal-Oxide-Semiconductor (CMOS)) process, where unlike analogue integrated circuits (ICs) using conventional CMOS processes, $iCMOS$ components can interact with bipolar input signals while providing increased performance, reduced power consumption and package size, which are crucial considering the nature of the project.

Considering the nature of this project, the noise in the signal needs to be minimise in order to ensure the accuracy of the signal sent into the EEG Signal Processing part so that the system can accurately interpret the users' thought.

As Nayak & Anilkumar states that the majority of EEG signals have a frequency of less than $200Hz$, although there are reports stated that EEG signals with a frequency of greater than $200Hz$ are associated with somatosensory stimulation and their sensitivity to vigilance states, motor interference or pharmacological manipulations, such as anesthetics or sedatives offer newer options for brain monitoring and diagnostics, which is neglectable given the nature of the project [3]. To only keep the

DOI: 10.54254/2753-8818/5/20230446

signals with a frequency of less than $200Hz$, a low pass filter (LPF) was implemented, the power spectrum of the LPF is shown below in Figure 4.

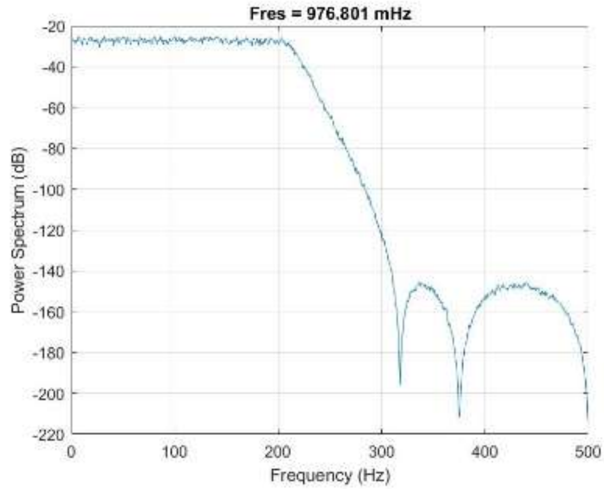

Figure 4. Power Spectrum of the LPF

The filter shown in Figure 4 above could be realized by a simple RC circuit shown in Figure 5 below.

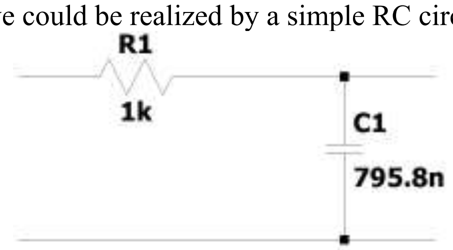

Figure 5. RC Circuit Realization of the LPF

The cut-off frequency of an RC circuit is given by

$$f = \frac{1}{2\pi R_1 C_1} = \frac{1}{2\pi * 1000\Omega * 795.8 * 10^{-9}F} = 200Hz \quad (1)$$

Leske & Dalal argued that $50Hz$ and $60Hz$ noise from the power outlet is one of the most major interferences during EEG signal processing [4]. Therefore, it is essential to use a notch filter or band stop filter to eliminate the interference. As all the experiment are conducted in Australia, where the electricity frequency is $50Hz$, so an $50Hz$ Infinite Impulse Response (IIR) filter was implemented. The magnitude response of the filter is shown below in Figure 6.

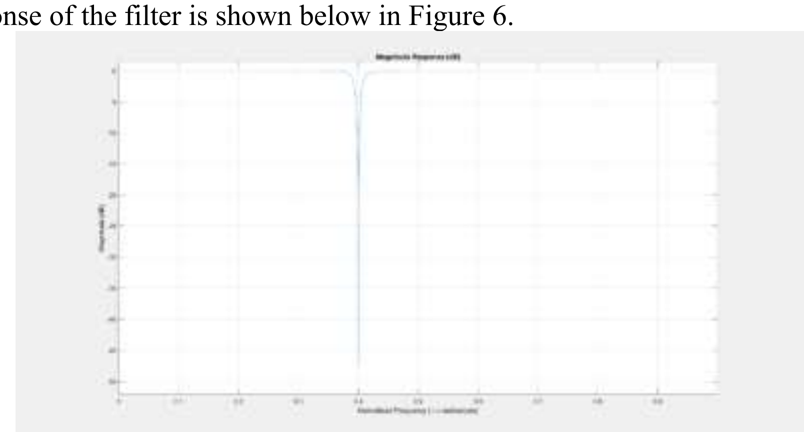

Figure 6. Magnitude Response of the Notch Filter.

The notch filter could be realized by the circuit below shown in Figure 7.

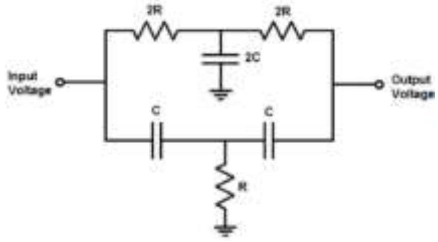

Figure 7. Notch Filter Circuit Realization

Where the notch frequency could be calculated by

$$f = \frac{1}{4\pi RC} \tag{2}$$

R was chosen to be $1k\Omega$ as a general value, C is calculated to be $1.592\mu F$.

2.1.2. Isolation circuit. An isolation circuit is also implemented to prevent the subsequent circuit from voltages and currents that endangers the circuit, which could also improve the stability of the system. Due to the long distance between the ADC and the motor drive system, the ground may be at different voltages. Through isolation, a potential difference is formed in the isolator instead of the sensitive circuit. The AD215 isolation circuit is used due to its high slew rate, fast transient response, high linearity, and low power consumption. The functional block diagram of AD215 is shown in Figure 8 below.

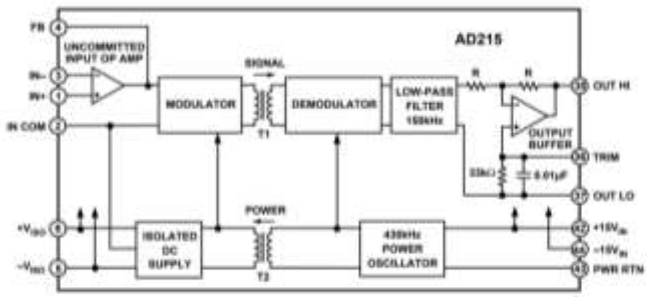

Figure 8. AD215 Isolation Circuit Functional Block Diagram.

2.1.3. EEG signal processing. In order to sort out the signals that were filtered before in section 2.1.1, as shown in Figure 9 below, firstly, a spike detection method is used to separate spikes from noise, then align the detected spikes to a common reference. Moreover, the aligned spiked need to be transformed into a certain set of features such as principal components etc. To reduce the dimensionality, the features that will be clustered in the subsequent process need to be identified. Finally, the spikes need to be classified into different groups (clusters) based on the extracted features [5].

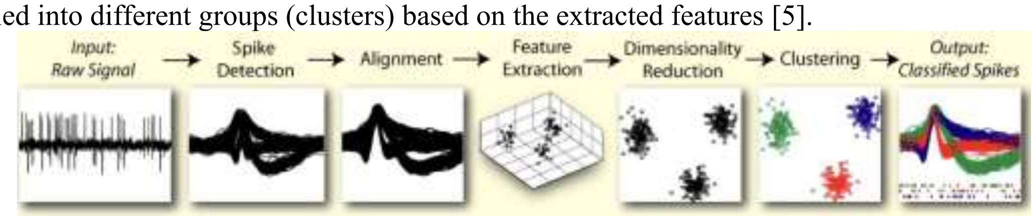

Figure 9. EEG Signal processing block diagram.

DOI: 10.54254/2753-8818/5/20230446

As it is highly machine learning and algorithm based, which is not the focus of this paper, it will not be fully addressed.

2.2. Microcontroller

The microcontroller takes in the classified EEG Signal and sends corresponding commands to the motor drive and control system. In order to ensure the normal functionality of the circuit, the ATMEGA328P microcontroller is chosen due to its low cost, low power consumption. sufficient I/O pins, high compatibility with Arduino and well documentation. The block diagram of ATMEGA328P is shown in Figure 10 below.

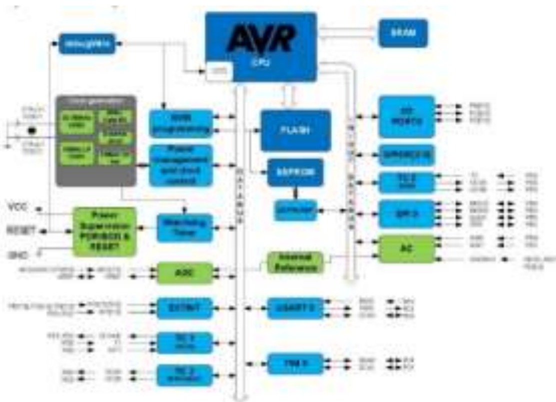

Figure 10. ATMEGA328P Block Diagram.

2.3. Motor driver

In order to realize what the user think, a robotic arm was implemented to do the corresponding actions. The robotic arm could be modelled by a motor.

2.3.1. Motor driver. The motor driver H-bridge module L293N, whose functional block diagram is shown in Figure 11 below, could be used as the motor driver.

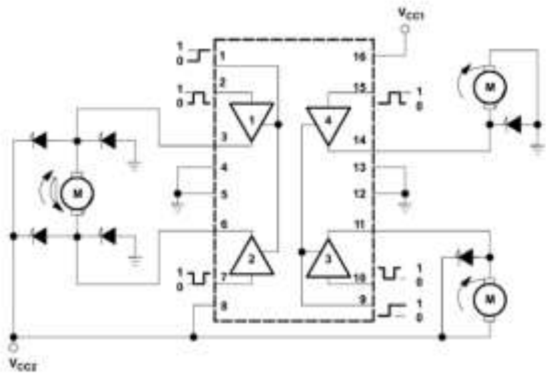

Figure 11. L293N Block Functional Diagram.

However, the $L293N$ module limits the output voltage to the motor to $5V$, which is not sufficient considering the nature of the project. Thus, a relay is considered to be used. Due to the control signal is a PWM signal, which indicates the relay needs to be turned on and off fast. Tuning on and off a relay is done by the metal physically connect to the terminals within the component. It could reduce the lifetime of the component and might defect the relay. Therefore, a motor driver made of a metal–oxide–semiconductor field-effect transistor (MOSFET) is implemented as shown in Figure 12 below. MOSFETs are made of semiconductors, which does not require frequent physical contact when being turned on and off.

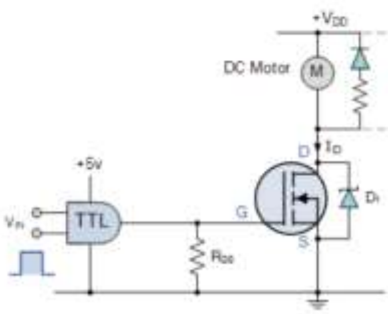

Figure 12. MOSFET Motor Driver Circuit Diagram.

MOSFET is the ideal device to interact with op-amps and logic gates because it has extremely high input and gate resistance, which allows it to achieve very high switching speed and it is easy to be driven simultaneously [6].

By exploiting the pulse-width modulation (PWM) output of Microcontroller ATMEGA328P, power MOSFETs can be used as DC motor speed controller. MOSFET switches with a PWM can be used as a DC motor speed controller which offers slick and silent motor operation since DC motors have high starting torque, which is proportional to its armature current. It could make the robotic arm more accurate, convenient to use, and increase the comfort for the patient to a large extent.

Since loads of DC motors are generally inductive, a flywheel diode is connected across the inductive load to dissipate any back electromotive force (emf) generated by the motor when the driver turns it "OFF". If this back emf is not dissipated, it could generate very large voltages which could potentially damage the electronic equipment. Faster switching and greater control of the peak reverse voltage and drop-out time can also be achieved by using a clamping network made up of a Zener diode connected in series with the diode. As a result, the reaction time can be quicker.

If additional security is required, a Zener diode D_1 could be connected between the drain and source region of the MOSFET to suppress over voltage switching transient and noise to provide extra protection to the MOSFET switch. Pull-down resistor R_{GS} is implemented to pull the transistor-to-transistor logic (TTL) output voltage down to $0V$ when the MOSFET is switched "OFF".

2.3.2. Motor controller. In order to prevent overshoot and improve the accuracy of the motor operation, a PID controller was implemented. In order to design a controller, system identification is conducted on the motor (robotic arm) to obtain the mathematical model of the motor. Bump test is one of the most used ways to do system identification. The bump test result is shown in Figure 13 below.

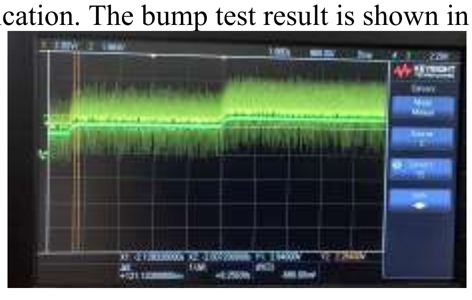

Figure 13. Bump Test Result of the Motor.

From Figure 13 above, $\Delta V = 0.54V$, time constant (τ) was set to $0.1s$. Therefore, the DC gain (K_{dc}) could be calculated by

$$\frac{\Delta V}{\Delta duty\ cycle} = \frac{0.54}{10} = 0.054 \tag{3}$$

As the motor could be roughly modelled as a first order system, the transfer function of the motor could be written as

$$G(S) = \frac{K_{dc}}{\tau s+1} = \frac{0.54}{s+1} \tag{4}$$

As the transient response is not the priority considering the nature of the project. Therefore, in order to improve the steady-state error, a PI controller is implemented as shown below in Figure 14.

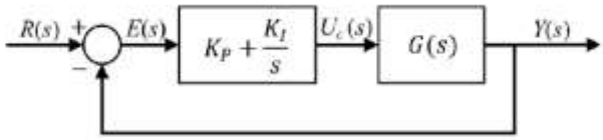

Figure 14. PI Controller.

where $R(s)$ is reference signal, $Y(s)$ is the output, $E(s)$ is the error signal. In order to make the system as fast and accurate as possible within the budget, we chose the percent overshoot ($\%OS$) to be 5% and the settling time (T_s) is 0.2s. Also, it could ensure the maximum smoothness of the motor operation.

Therefore, the tuned PI controller transfer function is

$$G_{c(s)} = 91 + \frac{1557}{s} \tag{5}$$

Experiment shows that its steady-state error is 2%, which means that it will deviate maximum 2% from its designed value. It shows the stability and accuracy of the motor control system. The PI Controller could be realized using the op-amp circuit shown in Figure 15 below [7].

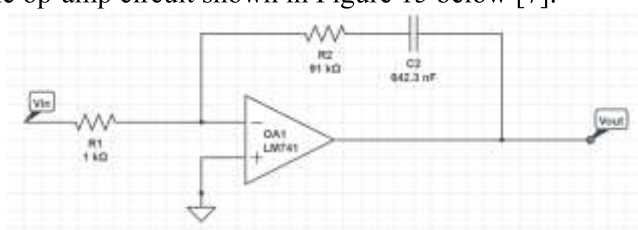

Figure 15. PI Controller Circuit Diagram.

In Figure 15, the input resistance R_1 is chosen to be $1k\Omega$ as a general value. The transfer function of the circuit shown in Figure 15 is

$$G_c(s) = -\frac{R_2}{R_1}\frac{(s+\frac{1}{R_2C_2})}{s} \tag{6}$$

After coefficient matching with the PI Controller transfer function, $R_2 = 91k\Omega$, $C_2 = 642.3pF$.

3. Software process

According to the difference in signal production principles, methods and processing algorithms processed by the system, the performance of the system and the applications are also different, but more and more researchers begin to pay attention to the EEG signal processing based on $ThinkGear^{TM}$ technology as the TGAM module in the $ThinkGear^{TM}$ technology could use a simple electrode to detect the weak EEG signal. Research and developments are being conducted now as well.

The P300 wave is an event-related potential (ERP) component elicited in the decision making process. Smaller occurrence probability of related events causes more significant P300 wave, especially in the parietal region of the head (middle or posterior), so the P300-based Brain Computer Interface (BCI) requires a small amount of pre-training. A typing tool introduced by Farwell and Donchin in 1988 used the P300 wave. A matrix is given to the patient with each entry of the matrix contains one letter of the English alphabet. The patient concentrates on the entry containing the letter need to be communicated while the rows and the columns of the matrix are highlighted. Each highlight is an event in the oddball sequence, the row and the column containing the attended cell are "rare" items and, therefore, only these events elicit a P300 wave. The computer thus detects the transmitted character by

DOI: 10.54254/2753-8818/5/20230446

determining which row and column elicited the P300. The experiment result shows an accuracy of 80% and a communicate rate of 7.8 characters per minute [8].

D.Xiao and W.Zhang had conducted thorough research on using TGAM Module in the $ThinkGear^{TM}$ technology on volume control of a speaker and a good result has been achieved [9]. The block diagram has been shown in Figure 16 below.

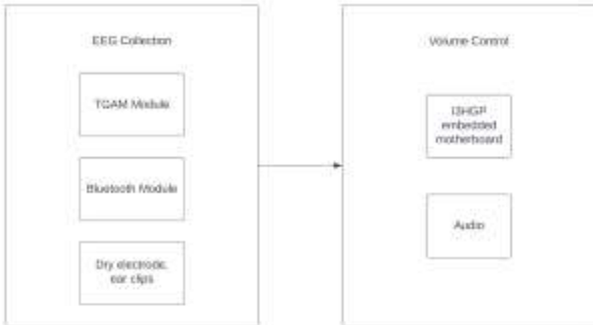

Figure 16. Block Diagram of Volume Control using TGAM Module.

J. Ji has also conducted research on using the decoded signal from the TGAM module to control the motor. In the experiment, the concentration rate is used to control the PWM duty cycle to control the rotation angle of the motor [10].

However, due to the space limitation of this paper, only theoretical analysis is conducted. Testing purpose experiment has been carried out.

3.1. EEG signal acquisition and processing

As mentioned in section 2.1, the EEG signal from the electrode will be first amplified and filtered, the converted to digital signal. After being converted to digital signal, it will go through detection, aligning, feature extracting and clustering. Then the classified signal will be sent to the microcontroller to control the robotic arm.

The low-pass filter (LPF) mentioned in section 2.1.1 could be realized by MATLAB function lowpass. Sample process block diagram is shown in Figure 17 below.

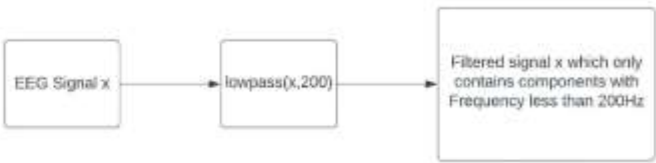

Figure 17. Sample LPF process block diagram.

The notch filter mentioned in section 2.1.1 could be realized by MATLAB function iirnotch. Sample process block diagram is shown in Figure 18 below.

Figure 18. Sample Process Block Diagram for Notch Filter in MATLAB.

In Figure 18 above, ω_0 is the notch frequency and BW is the $3dB$ bandwidth.

3.2. EEG signal processing

After the EEG signal is filtered and amplified, it could be further processed to interpret the users' thought. In order to interpret the signal accurately, there are five steps needed to be carried out, which are spike detection alignment, feature extraction, dimensionality reduction and clustering. As there are still noises which are not spikes even after filtering process, therefore, spike detection needs to be conducted to separate spikes from noise. Then the detected spikes need to be aligned to a common reference for further analysis. After that the features the spikes contain need to be extracted and choose the appropriate features to use in clustering. Finally, the spikes need to be classified into different clusters according to the extracted features. The block diagram of the whole process could be seen in Figure 9.

3.3. Robotic arm control

The robotic arm control is mainly realized by using MATLAB and Simulink. Due to the current resource limitation and complexity of the system, all the components have been simplified for the ease of understanding and calculation. The Simulink Model is shown in Figure 19 below for testing purpose. The system in reality is more complex that the system shown in Figure 19 below. In reality, the robotic arm that could best simulate the human's arm has 7 degrees of freedom.

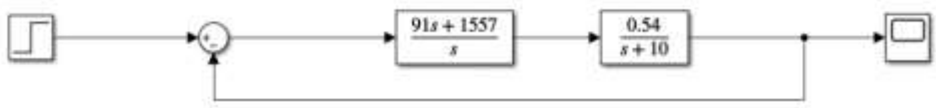

Figure 19. Simulink Model for PI Controller.

The motor speed control could be realized by using the analogWrite() function in Arduino, where duty cycle of the PWM signal could be varied to control the speed of the motor.

4. Conclusion

In this paper, a system that uses the users' EEG signal to control the movement of a robotic arm is designed. The system contains two parts, which are EEG Signal Acquisition and Processing, and Robotic Arm Driving and Control. The first part takes in EEG signal by placing electrodes on the users' head, then amplify, convert, filter and interpret the obtained EEG signal. Then the interpreted signal is sent to the second part where the microcontroller takes in the interpreted signal to control the robotic arm's behaviour. However, due to the limitations on the resource, only theoretical design and experiment for test purposes have been carried out. By designing such a system described in this paper, it could potentially change the way disabled people live and dramatically increase life quality of disabled people. In the future, a camera could be installed on the tip of the robotic arm to enable visual feedback, where it could help to increase the accuracy of the system. A robotic arm with more complex mechanism could also be used to increase the flexibility.

References

[1] People with disability in Australia, Prevalence of disability. (2022). Australian Institute of Health and Welfare. Retrieved October 22, 2022, from https://www.aihw.gov.au/reports/disability/people-with-disability-in-australia/contents/people-with-disability/prevalence-of-disability.

[2] Hosseini, S., Rajati, F., Ashtarian, H., Salari, N., Ghanbari, M., & Naghibifar, Z. (2018). Quality of life predictors in physically disabled people. Journal of Education and Health Promotion, 7(1), 61.

[3] Chetan S. Nayak, & Arayamparambil C. Anilkumar. (2021). EEG Normal Waveforms. StatPearls. https://europepmc.org/article/MED/30969627

[4] Leske, S., & Dalal, S. S. (2019). Reducing power line noise in EEG and MEG data via spectrum interpolation. NeuroImage, 189, 763–776. https://doi.org/10.1016/j.neuroimage.2019.01.026

[5] Gibson, S., Judy, J. W., & Markovic, D. (2012). Spike Sorting: The First Step in Decoding the Brain: The first step in decoding the brain. IEEE Signal Processing Magazine, 29(1), 124–143.

[6] Storr, W. (2022). MOSFET as a Switch - Using Power MOSFET Switching. Basic Electronics

Tutorials. Retrieved October 22, 2022, from https://www.electronics-tutorials.ws/transistor/tran_7.html

[7] Orman, K. (2022). Design of a Memristor-Based 2-DOF PI Controller and Testing of Its Temperature Profile Tracking in a Heat Flow System. IEEE Access, 10, 98384–98390. https://doi.org/10.1109/access.2022.3206022

[8] Farwell, L., & Donchin, E. (1988, December). Talking off the top of your head: toward a mental prosthesis utilizing event-related brain potentials. Electroencephalography and Clinical Neurophysiology, 70(6), 510–523.

[9] Xiao, D., & Zhang, W. (2015). Electroencephalogram based brain concentration and its human computer interface application. 2015 IEEE International Conference on Computer and Communications (ICCC). https://doi.org/10.1109/compcomm.2015.7387533

[10] Ji, J. (2017). Research on Manipulator Control Method Based on EEG Energy Decoding (Master's Thesis, Shenyang University of Technology).https://kns.cnki.net/KCMS/detail/detail.aspx?dbname=CMFD201702&filename=1017184818.nh